This is a preprint, the final version is subject to change, of the American Mineralogist (MSA)
Cite as Authors (Year) Title. American Mineralogist, in press.
(DOI will not work until issue is live.) DOI: http://dx.doi.org/10.2138/am-2017-6050

Revision 2

Single crystal X-ray structure analysis of the high-pressure $Mg_2Cr_2O_5$ phase with modified ludwigite-type structure

Takayuki Ishii[1,*], Noriyoshi Tsujino[2], Hidekazu Arii[1,†], Kiyoshi Fujino[3], Nobuyoshi Miyajima[4], Hiroshi Kojitani[1], Takehiro Kunimoto[3], Masaki Akaogi[1]

[1]Department of Chemistry, Gakushuin University, Mejiro, Toshima-ku, Tokyo 171-8588, Japan

[2]Institute for Study of the Earth's Interior, Okayama University, Misasa, Tottori 682-0193, Japan

[3]Geodynamics Research Center, Ehime University, Matsuyama, Ehime 790-8577, Japan

[4]Bayerisches Geoinstitut, University of Bayreuth, 95440 Bayreuth, Germany

*Present address: Bayerisches Geoinstitut, University of Bayreuth, 95440 Bayreuth, Germany

[†]Present address: Faculty of Education, University of Miyazaki, 1-1 Gakuen Kibanadai Nishi, Miyazaki, 889-2192 Miyazaki, Japan

Abstract

The crystal structure of the high-pressure $Mg_2Cr_2O_5$ phase was studied by single-crystal X-ray diffraction (XRD) analysis for the recovered samples. The 61 parameters including anisotropic

displacement parameters of each atom and site occupancies of Mg and Cr in cation sites were refined with R_1 = 1.26%, wR_2 = 4.33% and S_{fit} = 1.265 for 470 unique reflections. The results show that the structure of the recovered $Mg_2Cr_2O_5$ phase is the same as modified ludwigite (mLd)-type $Mg_2Al_2O_5$ (Space group: *Pbam* (no. 55)), and the lattice parameters are a = 9.6091(2) Å, b = 12.4324(2) Å, c = 2.8498(1) Å (Z = 4). The refined structure of the $Mg_2Cr_2O_5$ phase has four $(Mg,Cr)O_6$ octahedral sites and a MgO_6 trigonal prism site, and is similar to but distinct from that of $CaFe_3O_5$-type $Mg_2Fe_2O_5$ phase which has two octahedral sites and a bicapped trigonal prism site with two longer cation-oxygen bonds. The isotropic atomic displacement parameter of the trigonal prism site cation in mLd-type $Mg_2Cr_2O_5$ is relatively small compared with that of $CaFe_3O_5$-type $Mg_2Fe_2O_5$, suggesting that the trigonal prism site is less flexible for cation substitution than that of $CaFe_3O_5$-type structure. To stabilize mLd-type $A^{2+}{}_2B^{3+}{}_2O_5$ phase, it would be an important factor for the B^{3+} cation to have high octahedral-site preference, resulting in only A^{2+} cation being accommodated in the tight trigonal prism site. Our study also suggests that mLd-type phase with $(Mg,Fe^{2+})_2Cr_2O_5$ composition would crystallize as one of decomposed phases of chromitites, when the chromitites were possibly subducted into the mantle transition zone.

Keywords: Single crystal structure analysis, high pressure, modified ludwigite structure, chromite, $Mg_2Cr_2O_5$

Introduction

New high-pressure phases of $A^{2+}{}_2B^{3+}{}_2O_5$ stoichiometry have been recently reported: modified ludwigite (mLd)-type $Mg_2Al_2O_5$, $Fe_2Cr_2O_5$ and $Mg_2Cr_2O_5$ (*Pbam*) (Enomoto et al. 2009; Ishii et al. 2014; Ishii et al. 2015) and $CaFe_3O_5$ (or $Sr_2Tl_2O_5$)-type $Fe^{2+}{}_2Fe^{3+}{}_2O_5$ and $Mg_2Fe_2O_5$ (*Cmcm*) (Lavina et al. 2011; Evrard et al., 1980; Boffa Ballaran et al. 2015). These high-pressure phases are formed by decomposition of $A^{2+}B^{3+}{}_2O_4$ spinel-phases at high pressure. Fig. 1 shows mLd-type and $CaFe_3O_5$-type structures in $A_2B_2O_5$ composition. The mLd structure has four different $(A,B)O_6$ octahedral sites with partially disordered A^{2+} and B^{3+} and a AO_6 trigonal prism site in tunnel space surrounded by the edge- and corner-sharing octahedra. The $CaFe_3O_5$-type structure has a slightly different octahedral framework in which the coordination environment of cation in tunnel space is a trigonal prism with two longer cation-oxygen bonds. However, it is not clear what factors are important to stabilize mLd-type and $CaFe_3O_5$-type structures.

$MgCr_2O_4$ spinel is a dominant component of natural magnesium chromite. Chromian spinels containing high-pressure minerals (e.g. diamond and coesite) were discovered in chromitites in the Luobusa ophiolite, Tibet (Yang et al., 2007; Yamamoto et al., 2009; Dobrzhinetskaya et al., 2009). High-pressure and high-temperature phase relations in $MgCr_2O_4$ were investigated to examine the possible deep-mantle cycle of the chromitites by Ishii et al. (2015). They showed that at 12-15 GPa above 1100ºC, spinel-type $MgCr_2O_4$ first decomposes into a mixture of $Mg_2Cr_2O_5$ phase + Cr_2O_3

eskolaite. The two-phase assemblage changes to $CaTi_2O_4$-type $MgCr_2O_4$ at 17-19 GPa. Therefore, $Mg_2Cr_2O_5$ phase may be potentially one of *P-T* indicators for the chromitites derived from the mantle. Ishii et al. (2015) also showed that, with the Rietveld analysis of the powder X-ray diffraction data, the structure of the $Mg_2Cr_2O_5$ phase recovered from 15 GPa and 1600ºC is the mLd-type structure, which is the same as a high-pressure $Mg_2Al_2O_5$ phase first reported by Enomoto et al. (2009). However, atomic displacement parameters of all the atoms and cation occupancies in all the cation sites of the mLd-type $Mg_2Cr_2O_5$ have not been precisely determined.

In this study, to obtain more refined structure parameters of mLd-type $Mg_2Cr_2O_5$ and clarify the structural difference between mLd- and $CaFe_3O_5$-type structures, we have investigated the structure of the recovered $Mg_2Cr_2O_5$ phase based on the single crystal X-ray diffraction measurement. We discuss differences between the mLd-type and $CaFe_3O_5$-type structures and the stability of the mLd phase in natural chromitites in the deep mantle conditions.

Experimental methods

1. High-pressure syntheses and characterization

To synthesize the $Mg_2Cr_2O_5$ samples for single-crystal XRD measurement, a Kawai-type 6-8 multianvil high-pressure apparatus was used with tungsten carbide anvils of 5.0 mm truncated edge length in combination with pressure media of 5 wt% Cr_2O_3-doped MgO octahedra of 10 mm edge-length.

The single crystals of high-pressure $Mg_2Cr_2O_5$ phase were made from the mixture of MgO and $MgCr_2O_4$ of 1 : 1 molar ratio with a small amount of $Mg(OH)_2$. Addition of $Mg(OH)_2$ was made to obtain single crystals of $Mg_2Cr_2O_5$ large enough to analyze by single crystal XRD method. The starting material packed in a Pt capsule was placed in the central part of a $LaCrO_3$ heater in the octahedral pressure medium. The sample was held at 15 GPa and 1500ºC for 10 min, and then was kept at 15 GPa and 1300ºC for 1 h, using the multianvil apparatus at ISEI, Okayama University. Temperature of the central part of the sample was measured with a W-3%Re/W-25%Re thermocouple. Pressure effect on electromotive force of the thermocouple was ignored. A green single crystal of $Mg_2Cr_2O_5$ was picked up from the recovered run product, and was used for single-crystal XRD measurement.

The polycrystalline sample of $Mg_2Cr_2O_5$ phase was also synthesized to determine its lattice parameters by powder XRD method. A mixture of MgO and $MgCr_2O_4$ with the molar ratio of 1 : 1 was used as the starting material. The high-pressure synthesis and characterization of the $Mg_2Cr_2O_5$ polycrystalline sample were conducted with the same method as those in Ishii et al. (2015).

A micro-focus X-ray diffractometer (Rigaku RINT 2500V, MDG) with an X-ray beam collimated to 50 μm in diameter was used for phase identification of the recovered samples. The polycrystalline sample was identified using a powder X-ray diffractometer (Rigaku RINT 2500V) to confirm the single phase material and determine lattice parameters for $Mg_2Cr_2O_5$ phase. The X-ray diffraction measurements were conducted using monochromatized Cr Kα radiation operated at 45 kV

and 250 mA. The diffraction patterns were collected in a 2θ range of 10-140º.

A scanning electron microscope (SEM, JEOL JMS-6360) with an energy dispersive X-ray spectrometer (EDS, SGX Sensortech Sirius SD-10133) was used at acceleration voltage of 15 kV and probe current of 0.55 nA for composition analyses of the recovered samples. The standard materials for Mg and Cr were the natural forsterite and synthetic Cr_2O_3 eskolaite, respectively. The analyzed cation ratios of the sample synthesized for single crystal X-ray diffraction were Mg : Cr = 2.01(1) : 2.00(1).

2. Single crystal X-ray structure analysis

A single crystal of $Mg_2Cr_2O_5$ phase with dimensions of about 50 × 50 × 100 μm was used for the single crystal XRD measurement. The intensity data were collected up to 2θ = 54.80º with Mo Kα radiated from a rotating anode operated at 50 kV and 240 mA using a single-crystal X-ray diffractometer (Bruker AXS, Smart APEX2) equipped with a charge coupled device (CCD) detector at Gakushuin University. After empirical absorption correction using SADABS program (Sheldrick, 1996), the discrepancy factor among the equivalent reflections (R_{int}) was 1.62%. The modified ludwigite-type structure of $Mg_2Cr_2O_5$ determined by Ishii et al. (2015) was used as the initial structure for structure refinement, which was made by the SHELXL-97 program (Sheldrick, 1997) using the scattering factors of neutral atoms (International Tables for Crystallography, 1992). The structure was refined against $|F|^2$ by the full matrix least squares method. All the calculations for structure refinement were made using

the WinGX program (Farrugia, 2012). At the first stage of the refinement, the site occupancies of Mg and Cr in cation sites (M1-M4) and the isotropic displacement factors of all atoms were fixed to the values determined by Ishii et al. (2015). Then, the site occupancies of M1-M4 sites were refined with the constraint setting described subsequently. After the refinement of site occupancies, the anisotropic displacement factors were refined. At the final stage, all independent parameters were refined simultaneously.

Results and discussion

Table 1 summarizes the crystallographic data determined by the present single-crystal X-ray diffraction measurement of the $Mg_2Cr_2O_5$ phase with the reliability factors (R_{int}, R_1 and wR_2) and goodness-of-fit indicator (S_{fit}). Here, the lattice parameters obtained with a powder X-ray diffractometer with Bragg-Brentano geometry were used. In general, X-ray sources in a powder X-ray diffraction experiment (e.g. Cu, Co and Cr) have longer wavelengths and can measure *d* values to higher diffraction angle side than that in a single crystal X-ray diffraction experiment (Mo). Therefore, the lattice parameters derived from the power X-ray diffraction experiment are more reliable than those derived from the UB matrix of the single crystal X-ray diffraction experiment of the same sample because precision of *d* values at high diffraction angles is higher than that at low angles. The R_1 (1.26%), wR_2 (4.33%) and S_{fit} (1.265) values for 61 refined parameters converged to the sufficiently small values in

the final refinement and this result reveals that the refined structure of $Mg_2Cr_2O_5$ phase is reliable. Fig. 2 shows the obtained crystal structure of the $Mg_2Cr_2O_5$ phase. The refined structure ascertains that the recovered $Mg_2Cr_2O_5$ sample has the mLd-type structure reported by Enomoto et al. (2009). The structure of the mLd-type compound was, for the first time, determined by single crystal X-ray diffraction analysis. The refined structure parameters of mLd-type $Mg_2Cr_2O_5$ are summarized in Table 2 together with those obtained by the Rietveld analysis in Ishii et al. (2015). The atomic coordinates and the site occupancies by the present single crystal refinement are very close to those of the Rietveld refinement results of Ishii et al. (2015). However, the errors of the refined parameters are much smaller than those by the Rietveld refinement. In mLd-type $Mg_2Cr_2O_5$, there are four kinds of $(Mg,Cr)O_6$ octahedral sites (M1-M4) and a MgO_6 trigonal prism site (M5) in tunnel space formed by edge- and corner-shared M1-M4 sites. In the Rietveld analysis by Ishii et al. (2015), the occupancies of Mg and Cr in each site were estimated using the cation-oxygen distances and fixed in the refinement. Those site occupancies were carefully examined in the present study, where the site occupancies of Mg and Cr in the M1-M4 sites were refined using the atomic scattering factors of Mg and Cr under the restrained conditions that the total numbers of Mg and Cr in the unit cell are 4 and 8, respectively, and the M5 site was assumed to be occupied by only Mg. The assumption for the M5 site is based on trivalent chromium ion having relatively high preference for octahedral sites, due to its high crystal-field stabilization energy (O'Neill and Navrotsky, 1984). We verified that attempts at refining Cr in the M5 site result in a larger

R_1 value. We also obtained more accurate atomic displacement parameters of each atom than those by Rietveld analysis of Ishii et al. (2015). The equivalent isotropic displacement parameters, U_{eq}, of M1-M5 site cations are much smaller than those of Ishii et al. (2015). The feature of mLd-type structure is shown in the atomic displacement of M5 site cation, which is larger (0.0085 $Å^2$) than those of M1-M4 ones (0.0040-0.0065 $Å^2$), because the M5 trigonal prism site is in the relatively large tunnel space formed by the edge- and corner-sharing MO_6 octahedra. Table 3 shows the interatomic distances and angles in the refined mLd-type structure of $Mg_2Cr_2O_5$. In the M1-M4 sites, average cation-oxygen distances (2.014-2.062 Å) are smaller than Mg-O bond length and almost same as or larger than Cr-O estimated from the effective ionic radii of Mg^{2+} (0.72 Å), Cr^{3+} (0.615 Å) and O^{2-} (1.40 Å) for six-fold coordination by Shannon (1976). Among the M1-M4 sites, the average cation-oxygen distances increase with the decrease of the site occupancy of Cr. The average Mg-O bond length of MgO_6 trigonal prism is 2.141 Å, which is close to 2.12 Å calculated from the effective ionic radii of Mg^{2+} and O^{2-}.

The structural features of mLd-type $Mg_2Cr_2O_5$ in this study and $CaFe_3O_5$-type $Mg_2Fe_2O_5$ reported by Boffa Ballaran et al. (2015) are compared, based on their structure parameters as follows. Fig. 3 shows thermal ellipsoids of atoms in both of the structures. In the mLd-type phase, the anisotropic atomic displacement parameters, U_{aniso}, of the M5 trigonal prism site show that U_{22} is the largest (Table 2), which means that M5 site cation anisotropically vibrates almost along *b* axis (Fig. 3a) although a part of the anisotropic ellipsoid shape effect may be due to static disorder. This is explained by the

oxygen-oxygen distances in the trigonal prism site as follows. The square space surrounded by four oxygen atoms (two O1 and two O3) in this site is the largest of the three because O1-O3 distance (2.881 Å) is larger than O1-O5 (2.694 Å) and O3-O5 distances (2.696 Å), which means that the largest square space direction is relatively flexible for the cation. On the other hand, in $CaFe_3O_5$-type $Mg_2Fe_2O_5$ (Fig. 3b), the thermal ellipsoid of the trigonal prism site cation is enlarged approximately along the *c*-axis, which corresponds to the direction of two longer cation-oxygen bonds, because two oxygen-oxygen distances (2.840 Å) to the *c*-axis direction in this site are longer than the other (2.660 Å). Additionally, thermal ellipsoids of the oxygen in two longer cation-oxygen bonds are elongated to the trigonal prism site cation. These features are consistent with the structural difference between the two phases: the trigonal prism site of $CaFe_3O_5$-type $Mg_2Fe_2O_5$ has two additional longer cation-oxygen bonds to form the bicapped trigonal prism, whereas that of mLd-type $Mg_2Cr_2O_5$ does not have them. Furthermore, the U_{eq} for cations in $(Mg,Fe^{3+})O_6$ trigonal prism site (0.0154 $Å^2$) of $CaFe_3O_5$-type $Mg_2Fe_2O_5$ is much larger than that of mLd-type $Mg_2Cr_2O_5$ even though the average cation-oxygen bond length of the trigonal prism site of the former (2.169 Å) is almost same as the latter (2.141 Å). This suggests that the cation in the trigonal prism site in $Mg_2Cr_2O_5$ phase is more confined than that in $Mg_2Fe_2O_5$ phase without two longer cation-oxygen bonds. Additionally, Siersch et al. (2017) reported compressibility of $Mg_2Fe_2O_5$ phase and that the *c* axis is the most compressible direction probably because of flexibility of an M-O-M angle by corner-sharing octahedra (Fig. 3). $Mg_2Fe_2O_5$ phase has an octahedral framework with a mirror

plane perpendicular to the *c* axis and corner-sharing octahedra along the *b* axis (Fig. 1), which makes the flexible M-O-M angle to the *c* axis and the flexible octahedral tunnel space. On the other hand, $Mg_2Cr_2O_5$ phase does not have such a symmetrical octahedral framework and a corner-sharing arrangement (Fig. 1). This also supports that the $Mg_2Cr_2O_5$ phase has a tighter trigonal prism site. Therefore, it would be reasonably described that the M5 site in mLd-type $Mg_2Cr_2O_5$ has relatively tight trigonal prism environment against the more flexible 6 + 2 coordination (bicapped trigonal prism) site in $CaFe_3O_5$-type $Mg_2Fe_2O_5$. Fe^{3+} has no octahedral site preference because of zero crystal field stabilization energy, and therefore $Mg_2Fe_2O_5$ phase may prefer the $CaFe_3O_5$-type structure having a relatively flexible bicapped trigonal prism site in which Fe^{3+} is accommodated with Mg^{2+}-Fe^{3+} disordering. Instead, only Mg^{2+} is accommodated in the trigonal prism site of mLd-type $Mg_2Cr_2O_5$ phase, and Cr^{3+} and Mg^{2+} occupy the octahedral sites due to the octahedral preference of Cr^{3+}. Considering the above issues and the fact that $Fe_2Cr_2O_5$ crystallizes in the mLd structure (Ishii et al., 2014), it could be concluded that an important factor for stabilizing mLd-type $A^{2+}{}_2B^{3+}{}_2O_5$ phase is that B^{3+} cation has high octahedral-preference and, as the result, only A^{2+} cation is accommodated in the tight trigonal prism site. This would also explain why $Mg_2Al_2O_5$ has mLd-type structure because Al^{3+} has too small ion radius for the trigonal prism site and would prefer the octahedral sites.

Implication

In this study, we have demonstrated that high-pressure $Mg_2Cr_2O_5$ phase has the mLd-type structure by single crystal X-ray structure refinement. The structural features of the mLd-type $Mg_2Cr_2O_5$ suggest that it is less flexible for the incorporation of other components, compared with the $CaFe_3O_5$-type. Here, we discuss on the composition and stability of mLd phase in natural chromitites recycled in the mantle. As discussed in Ishii et al. (2014, 2015), mLd-type phase may possibly be a good petrogenetic indicator of *P-T* conditions for ultra-high pressure chromitites. To constrain the *P-T* history of the ultra-high pressure chromitites recycled in the mantle, it is necessary to properly evaluate the stability field of mLd-type phase. It is considered that most of natural chromitites have compositions approximately in the $(Mg,Fe)_2SiO_4$-$(Mg,Fe)Cr_2O_4$ system. Therefore, it is important to consider effects of incorporation of Fe and Si components into $Mg_2Cr_2O_5$ on the stability field of mLd-type phase. Ishii et al. (2014, 2015) showed that the stability pressure ranges of both the mLd-type $Mg_2Cr_2O_5$ and $Fe_2Cr_2O_5$ in $MgCr_2O_4$ and $FeCr_2O_4$ systems, respectively, are very similar, 12-18 GPa at 1400-1600°C, which are mostly the upper part of the mantle transition zone (MTZ) conditions (Akaogi et al. 1989). Therefore, it is expected that $(Mg,Fe)_2Cr_2O_5$ continuous solid solution is formed in the upper part of MTZ conditions. The possible incorporation of Fe^{3+} in mLd-type $Mg_2Cr_2O_5$ has been poorly understood. Although further experimental study is necessary to clarify how much Fe^{3+} can accommodate in the mLd-type structure, large amounts of Fe_4O_5 and $Mg_2Fe_2O_5$ components might not incorporate into $(Mg,Fe)_2Cr_2O_5$ phase in chromitites recycled from the MTZ. This is because the mLd structure is less

flexible for incorporation of Fe^{3+}, as discussed above, and also because the fO_2 in MTZ could be just below iron-wüstite buffer condition and the $Fe^{3+}/\sum Fe$ ratio would be very low (e.g. ~3%) (Frost and McCammon, 2008). On the other hand, in the $MgCr_2O_4$-Mg_2SiO_4 system, Bindi et al. (2015, 2016) synthesized the mineral assemblage of mLd-type $Mg_2Cr_2O_5$ + Cr-bearing minerals such as eskolaite, garnet, anhydrous phase B and a distorted orthorhombic $CaTi_2O_4$-type phase at 12 and 16 GPa at 1600°C. Presence of large amounts of garnet and anhydrous phase B in the mineral assemblage of Bindi et al. would suggest that most Si component was incorporated into the silicate phases rather than mLd phase. Therefore, we suggest that, when chromitites are subdcuted into the upper part of MTZ, the mLd-type phase with dominant $(Mg,Fe)_2Cr_2O_5$ composition coexists with other Cr-bearing minerals and silicates and that the trace mLd-type $(Mg,Fe)_2Cr_2O_5$ would remain in the chromitites recycled from the MTZ. However, the occurrence of the mLd-type $(Mg,Fe)_2Cr_2O_5$ in the chromitites has not been reported yet. Therefore, we suggest that the ultra-high-pressure chromitites discovered so far have experienced the mantle conditions down to at most about 360-390 km depth (12-13 GPa). This is because the lower pressure limit of the stability field of mLd-type $(Mg,Fe)_2Cr_2O_5$ is 12-13 GPa at mantle temperature of 1300-1600°C (Ishii et al., 2014, 2015).

Acknowledgements

We thank H. Ohfuji, T. Irifune and T. Kuribayashi for useful discussions, and K. Mochida for

his help with single-crystal structure analysis. We are grateful to reviewers for constructive comments and valuable suggestions. This research was partly supported by the Grants-in-Aid (nos. 22340163, 25287145 and 17H02986 to M. Akaogi) of the Scientific Research of the Japan Society for the Promotion of Science (JSPS) and the Research Fellowship from JSPS for Young Scientists to T. Ishii, and by the MEXT-Supported Program for the Strategic Research Foundation at Private Universities.

References cited

Akaogi, M., Ito, E., and Navrotsky, A. (1989). Olivine-modified spinel-spinel transitions in the system Mg_2SiO_4-Fe_2SiO_4: Calorimetric measurements, thermochemical calculation, and geophysical application. Journal of Geophysical Research: Solid Earth, 94, 15671-15685.

Bindi L., Sirotkina E., Bobrov A.V., and Irifune T. (2015). Structural and chemical characterization of $Mg[(Cr,Mg)(Si,Mg)]O_4$, a new post-spinel phase with sixfold-coordinated silicon. American Mineralogist, 100, 1633–1636.

Bindi, L., Sirotkina, E.A., Bobrov, A.V., Nestola, F., and Irifune, T. (2016). Chromium solubility in anhydrous Phase B. Physics and Chemistry of Minerals, 43, 103-110. DOI 10.1007/s00269-015-0777-2

Boffa Ballaran, T., Uenver-Thiele, L., and Woodland, A. B. (2015) Complete substitution of Fe^{2+} by Mg in Fe_4O_5: The crystal structure of the $Mg_2Fe_2O_5$ end-member. American Mineralogist, 100, 628-632.

DOI: 10.2138/am-2015-5138.

Dobrzhinetskaya, L., Wirth, R., Yang, J.-S., Hutcheon, I., Weber, P., and Green, H.W. (2009). High pressure highly reduced nitride sand oxides from chromite of a Tibetan ophiolite. Proc. Natl. Acad. Sci. USA 106, 19233–19238.

Enomoto, A., Kojitani, H., Akaogi, M., and Yusa, H. (2009) High-pressure transitions in $MgAl_2O_4$ and a new high-pressure phase of $Mg_2Al_2O_5$. Journal of Solid State Chemistry, 182, 389-395, doi:10.1016/j.jssc.2008.11.015.

Evrard, O., Malaman, B., Jeannot, F., Courtois, A., Alebouyeh, H., and Gerardin, R. (1980) Mise en évidence de $CaF^2e_4O_6$ et détermination des structures cristallines des ferrites de calcium $CaFe_{2+n}O_{4+n}$(n = 1, 2, 3): nouvel exemple d'intercroissance. Journal of Solid State Chemistry, 35, 112-119.

Farrugia, L.J. (2012) WinGX and ORTEP for Windows: an update Journal of Applied Crystallography, 45, 849-854.

Frost, D.J., and McCammon, C.A. (2008) The redox state of Earth's mantle. Annual Review of Earth and Planetary Sciences, 36, 389-420.

Ishii, T., Kojitani, H., Tsukamoto, S., Fujino, K., Mori, D., Inaguma, Y., Tsujino, N., Yoshino, T., Yamazaki, D., Higo, Y., Funakoshi, K., and Akaogi, M. (2014) High-pressure phase transitions in $FeCr_2O_4$ and structure analysis of new post-spinel $FeCr_2O_4$ and $Fe_2Cr_2O_5$ phases with meteoritical and

petrological implications. American Mineralogist, 99, 1788-1797. DOI: 10.2138/am.2014.4736.

Ishii, T., Kojitani, H., Fujino, K., Yusa, H., Mori, D., Inaguma, Y., Matsushita, Y., Yamaura, K., and Akaogi, M. (2015) High-pressure high-temperature transitions in $MgCr_2O_4$ and crystal structures of new $Mg_2Cr_2O_5$ and post-spinel $MgCr_2O_4$ phases with implications for ultra-high pressure chromitites in ophiolites, American Mineralogist, 100, 59-65. DOI: 10.2138/am.2014.4736.

Lavina, B., Dera, P., Kim, E., Meng, Y., Downs, R.T., Weck, P.F., Sutton, S.R., and Zhao, Y. (2011) Discovery of the recoverable high-pressure iron oxide Fe_4O_5. Proceedings of the National Academy of Sciences, 108, 17281-17275, doi/10.1073/pnas.1107573108.

O'Neill, H. St. C. and Navrotsky, A. (1984) Cation distributions and thermodynamic properties of binary spinel solid solutions. American Mineralogist, 69, 733-753.

Shannon, R.D. (1976) Revised effective ionic radii and systematic studies of interatomic distances in halides and chalcogenides. Acta Crystallographica, A32, 751-767.

Sheldrick, G.M. (1996) SADABS. Program for empirical absorption correction of area detector data. Institut für Anorganische Chemie, University of Göttingen, Germany.

Sheldrick, G.M. (1997) SHELX-97 (computer program), University of Göttingen, Germany.

Siersch, N.C., Ballaran, T.B., Uenver-Thiele, L., and Woodland, A.B. (2017). Compressibility and high-pressure structural behavior of $Mg_2Fe_2O_5$. American Mineralogist, 102, 845-850.

Wilson, A.J.C., Eds. (1992) International Tables for Crystallography, vol. C, Dodrecht: Kluwer

Academic Publishers.

Yamamoto, S., Kojima, T., Hirose, K., and Maruyama, S. (2009) Coesite and clinopyroxene exsolution lamella in chromites: *In-situ* ultrahigh-pressure evidence from podiform chromitites in the Luobusa ophiolite, southern Tibet. Lithos, 109, 314-322.

Yang, J.S., Dobrzhinetskaya, L., Bai, W.J., Fang, Q.S., Robinson, P.T., Zhang, J., and Green, H.W. (2007) Diamond- and coesite-bearing chromitites from the Luobusa ophiolite, Tibet. Geology, 35, 875-878, doi: 10.1130/G23766A.

Figure captions

Figure 1. Crystal structures of (a) modified ludwigite (mLd)-type structure (space group and setting: *Pbam* (*a b c*)) and (b) $CaFe_3O_5$-type $A_2B_2O_5$ (space group and setting: *Cmcm* (*a b c*)). Both unit cells are shown by solid lines. Larger and smaller spheres represent cations and oxygen, respectively.

Figure 2. (a) Crystal structure, (b) thermal-ellipsoid model and (c) coordination environments of each site of $Mg_2Cr_2O_5$ high-pressure phase determined by single crystal X-ray diffraction analysis. Squares in (a) and (b) show unit cell. Different color areas in the spheres of M1-M4 sites show the ratio of Mg and Cr (See Table 2.).

Figure 3. (a) Tunnel structures, trigonal prism sites and thermal ellipsoids in modified ludwigite (mLd)-type $Mg_2Cr_2O_5$ (space group and setting: *Pbam* (*a b c*)) in this study and (b) $CaFe_3O_5$-type $Mg_2Fe_2O_5$ (space group and setting: *Cmcm* (*a b c*)) reported by Boffa Ballan et al. (2015). Dashed lines represent oxygen-oxygen distances. Thermal ellipsoids in oxygen octahedra and trigonal prisms represent cations. M-O-M represents an angle between two corner-sharing octahedra.

Table 1. Crystallographic data of $Mg_2Cr_2O_5$.

Crystal color	Green
Crystal system	Orthorhombic
Lattice parameter	a = 9.6091(2) Å
	b = 12.4324(2) Å
	c = 2.8498(1) Å
	V = 340.44(1) Å^3
Z	4
Space group	*Pbam* (no. 55)

Chemical composition*	$Mg_{2.00(1)}Cr_{2.00(1)}O_5$
Measurement temperature	298 K
Measured/unique reflections	3885/470
Index ranges	$-12 \le h \le 12$
	$-16 \le k \le 16$
	$-3 \le l \le 3$
2θ max	54.80°
R_{int}	0.0162
R_1	0.0126
wR_2	0.0433
Goodness-of-fit (S_{fit})	1.265

$R_{int} = \Sigma \mid |F_o|^2 - |F_o|^2(\text{mean}) \mid / \Sigma |F_o|^2$, $R_1 = \Sigma \mid |F_o| - |F_c| \mid / \Sigma |F_o|$, $wR_2 = \{\Sigma w (|F_o|^2 - |F_c|^2)^2 / \Sigma| F_o|^2\}^{1/2}$, $S_{fit} = \{\Sigma w (|F_o|^2 - |F_c|^2)^2 / (n - p)\}^{1/2}$, $w = 1 / \{\sigma^2 (|F_o|^2) + (0.0227 \times P)^2 + 0.2911 \times P\}$ and $P = ([\text{Maximum } (|F_o|^2 \text{ or } 0)] + 2 \times |F_c|^2) / 3$,

where F_o and F_c are the observed and calculated structure factors, respectively. w, n and p, are the statistical weight, the number of reflections and the total number of parameters refined, respectively. Maximum (F_o^2 or 0) is replaced by 0 when the observed F_o^2 value is negative because the background is higher than the peak.

*Chemical composition calculated from site occupancies of Mg and Cr.

This is a preprint, the final version is subject to change, of the American Mineralogist (MSA)
Cite as Authors (Year) Title. American Mineralogist, in press.
(DOI will not work until issue is live.) DOI: http://dx.doi.org/10.2138/am-2017-6050

Table 2. Structure parameters of modified ludwigite-type $Mg_2Cr_2O_5$.

Atom	Wyckoff site	*x*	*y*	*z*	*g* (Mg)	*g* (Cr)	U_{11}
	U_{22}	U_{33}	U_{23}	U_{13}	U_{12}	U_{eq}	
M1	2*a*	0	0	0	0.288(5)	0.712(5)	0.0025(3)
	0.0053(3)	0.0041(3)	0	0	−0.0002(2)		0.0040(2)
		0	0	0	0.3	0.7	
M2	2*d*	0	1/2	1/2	0.906(5)	0.094(5)	0.0052(5)
	0.0061(5)	0.0080(6)	0	0	−0.0003(3)		0.0065(4)
		0	1/2	1/2	0.8	0.2	
M3	4*g*	0.02049(4)	0.28839(3)	0	0.263(3)	0.737(3)	0.0031(2)
	0.0049(2)	0.0043(2)	0	0	0.0003(1)	0.0041(2)	
		0.0221(2)	0.2824(1)	0	0.35	0.65	
M4	4*h*	0.27072(4)	0.38466(3)	1/2	0.145(3)	0.855(3)	0.0030(2)
	0.0050(2)	0.0042(2)	0	0	−0.0003(1)		0.0041(2)
		0.2730(1)	0.3827(1)	1/2	0.1	0.9	
M5	4*g*	0.24330(8)	0.13245(7)	0	1 [a]	0 [a]	0.0059(4)
	0.0128(4)	0.0067(4)	0	0	−0.0020(3)		0.0085(2)

		0.2432(2)	0.1306(2)	0	1	0	
O1	4*h*	0.1411(2)	0.0307(1)	1/2	-	-	0.0049(7)
	0.0056(7)	0.0055(7)	0	0	−0.0001(6)		0.0053(3)
		0.1423(6)	0.0237(5)	1/2	-	-	
O2	4*g*	0.4078(2)	0.3494(1)	0	-	-	0.0060(7)
	0.0083(8)	0.0068(8)	0	0	0.0011(6)	0.0070(3)	
		0.4115(5)	0.3510(5)	0	-	-	
O3	4*h*	0.4033(2)	0.1431(1)	1/2	-	-	0.0039(7)
	0.0070(7)	0.0060(8)	0	0	−0.0003(6)		0.0056(3)
		0.4103(5)	0.1424(5)	1/2	-	-	
O4	4*g*	0.1322(2)	0.4318(1)	0	-	-	0.0059(7)
	0.0085(8)	0.0068(8)	0	0	0.00011(6)		0.0071(3)
		0.1373(6)	0.4296(5)	0	-	-	
O5	4*h*	0.1569(2)	0.2470(1)	1/2	-	-	0.0054(7)
	0.0062(7)	0.0065(7)	0	0	0.0004(6)	0.0060(3)	
		0.1598(6)	0.2488(4)	1/2	-	-	

Notes: The anisotropic displacement factor exponent is $\exp\{-2\pi^2[h^2(a^*)^2U_{11} + k^2(b^*)^2U_{22} +$

$l^2(c^*)^2U_{33} + 2klb^*c^*U_{23} + 2hla^*c^*U_{13} + 2hka^*b^*U_{12}]\}$. g (Mg) and g (Cr) are site occupancies of Mg and Cr, respectively. The equivalent isotropic atomic displacement parameter U_{eq} is calculated from $1/3[U_{11}\ (aa^*)^2 + U_{22}\ (bb^*)^2 + U_{33}\ (cc^*)^2 + 2U_{23}\ b^*c^*bc + 2U_{13}\ a^*c^*ac + 2U_{12}\ a^*b^*ab]$.

The fractional coordinates and site occupancies determined by Rietveld analysis in Ishii et al. (2015) are written under the present data of each site to compare with those by single crystal structure analysis in this study.

[a]Fixed value.

[b]Isotropic atomic displacement parameters of all of oxygen were refined with the common value.

Table 3. Interatomic distances and angles in modified ludwigite-type $Mg_2Cr_2O_5$.

Bond length (Å)					
M1 site		M2 site		M3 site	M4 site
M1-O1×4	2.003(1)	M2-O3×2	2.008(2)	M3-O2	
	2.027(2)	M4-O1[i]	2.004(2)	M5-O1×2	
	2.144(1)				

M1-O2×2	2.071(2)	M4-O4×4	2.089(1)	M3-O4		
	2.081(2)	M4-O5	2.031(2)	M5-O3^{ii}×2		
	2.100(1)					
Average	2.026	Average	2.062	M3-O3×2		
	2.006(1)	M4-O2^{ii}×2	1.989(1)	M5-O5×2		
	2.179(1)					
n_c	5.95	n_c	5.92	M3-O5×2		
	2.004(1)	M4-O4×2	2.036(1)	Average	2.141	
BVS	2.45	BVS	2.23	Average	2.021	Averag
				n_c	5.96	n_c
				BVS	2.48	BVS

Bond angles (°)

O1^{ii}-M1-O1	89.32(8)	O1-M1-O1	90.68(8)	O2^{iii}-M1-O2	
	180.0(1)	O4-M2-O4	86.03(6)	O4-M2-O4^{ii}	
	93.97(6)	O3-M2-O3^{ii}	180.0(1)	O3-M3-O5	

	88.36(7)	O5-M3-O5	90.67(9)	O3-M3-O3		
	90.51(8)	O2-M3-O4	178.7(1)			
O2-M4-O2	91.5(1)	O4-M4-O4	88.82(9)	$O1^{i}$-M4-O5		
	172.5(1)					
M4-$O2^{ii}$-M4	91.5(1)	M3-$O2^{ii}$-$M4^{ii}$	122.68(3)	$M1^{i}$-$O2^{ii}$-M4		
	94.84(3)	M4-O4-M4	88.8(1)	M3-O4-M4		
	95.21(4)					
M4-O4-M2	92.12(3)	$M1^{i}$-$O1^{i}$-M4	96.53(4)	M3-O5-M4		
	97.81(4)	$M3^{i}$-O2-$M4^{iii}$	122.68(3)	M3-O5-M3	90.7(1)	
M2-O4-M3	91.97(9)	M3-O3-M3	90.5(1)	M2-O3-M3	96.7(1)	M1-O1

Abbreviations: n_c: effective coordination number; BVS: bond valence sum value.

Symmetry codes: (i) -x+1/2, y+1/2, -z (ii) x+1/2, -y+1/2, z (iii) -x, -y, -z.

This is a preprint, the final version is subject to change, of the American Mineralogist (MSA)
Cite as Authors (Year) Title. American Mineralogist, in press.
(DOI will not work until issue is live.) DOI: http://dx.doi.org/10.2138/am-2017-6050

Fig. 1

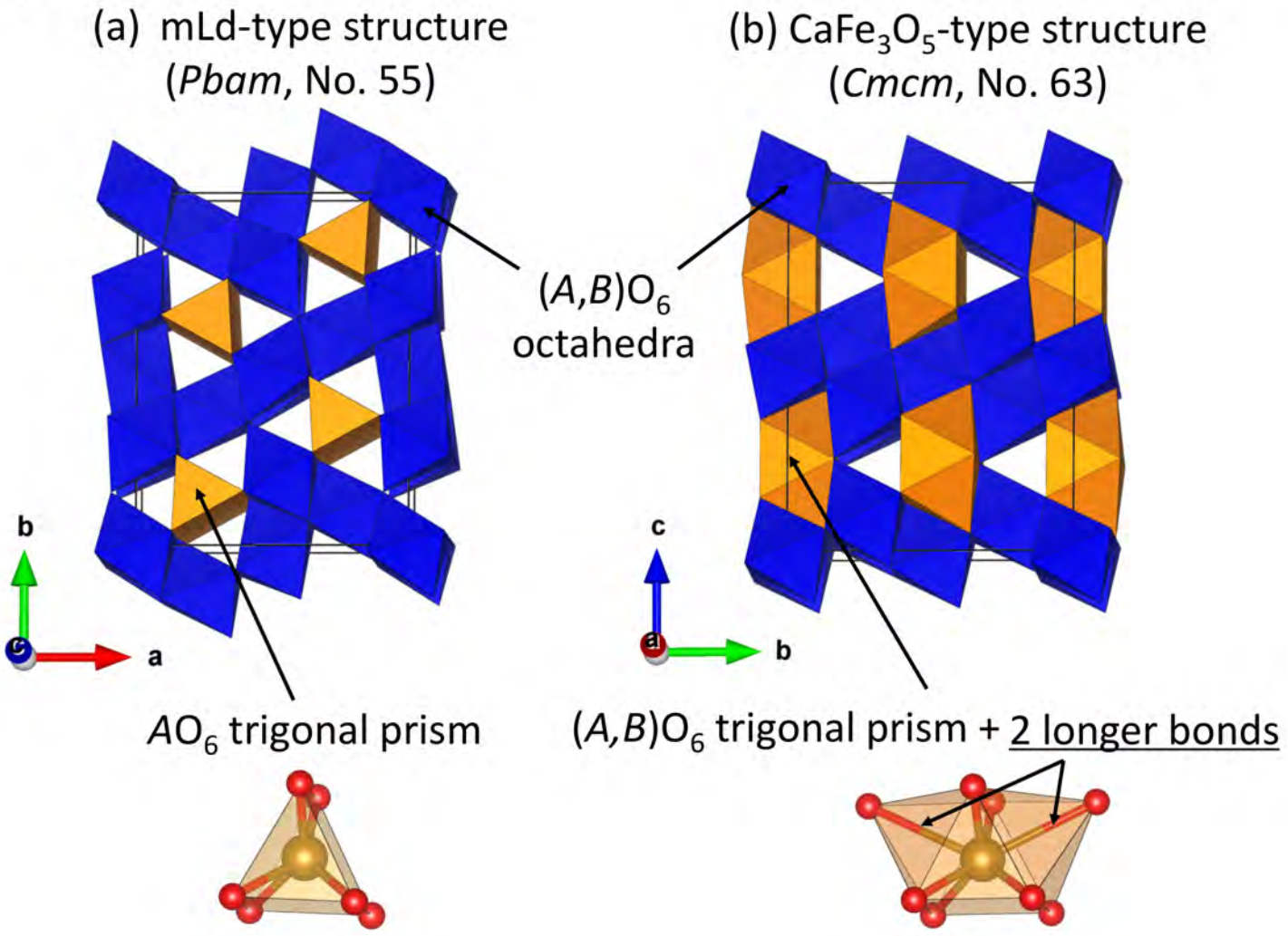

This is a preprint, the final version is subject to change, of the American Mineralogist (MSA)
Cite as Authors (Year) Title. American Mineralogist, in press.
(DOI will not work until issue is live.) DOI: http://dx.doi.org/10.2138/am-2017-6050

Fig. 2

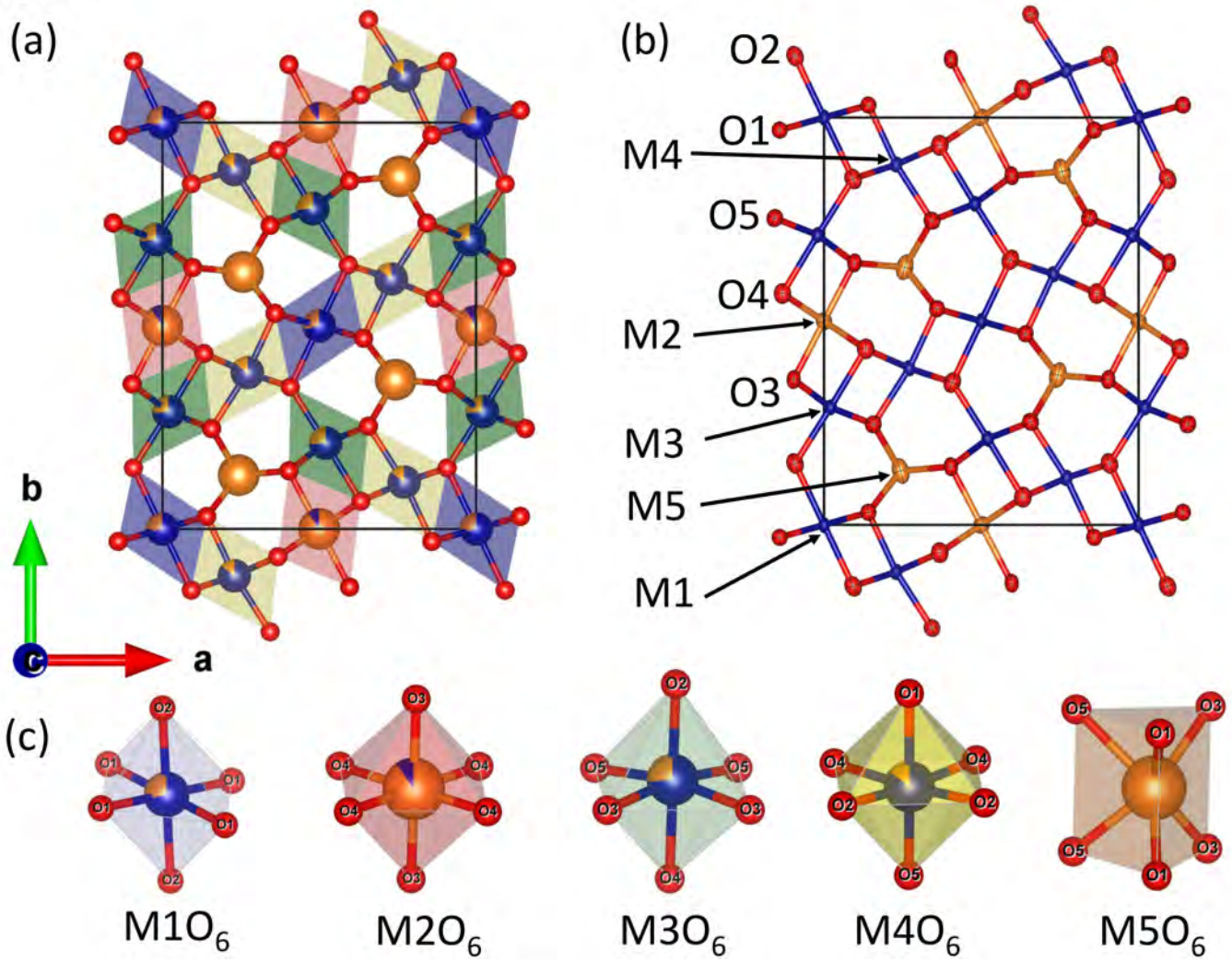

This is a preprint, the final version is subject to change, of the American Mineralogist (MSA)
Cite as Authors (Year) Title. American Mineralogist, in press.
(DOI will not work until issue is live.) DOI: http://dx.doi.org/10.2138/am-2017-6050

Fig. 3